OAK RIDGE
NATIONAL LABORATORY
MANAGED BY UT-BATTELLE
FOR THE DEPARTMENT OF ENERGY

ORNL/TM-2007/033

Assessment of Cavitation-Erosion Resistance of Potential Pump Impeller Materials for Mercury Service at the Spallation Neutron Source

MARCH 2007

S. J. Pawel

UT-BATTELLE

ORNL/TM-2007/033

Materials Science and Technology Division

Assessment of Cavitation-Erosion Resistance of Potential Pump Impeller Materials for Mercury Service at the Spallation Neutron Source

S. J. Pawel

Date Published: March 2007

Prepared for the
U.S. Department of Energy
Spallation Neutron Source

Prepared by
OAK RIDGE NATIONAL LABORATORY
Oak Ridge, Tennessee 37831-6285
Operated by
UT-Battelle, LLC
for the
U. S. DEPARTMENT OF ENERGY
Under contract DE-AC05-00OR22725

CONTENTS

LIST OF TABLES

FIGURES

ABSTRACT

Using a standard vibratory horn apparatus, the relative cavitation-erosion resistance of a number of cast alloys in mercury was evaluated to facilitate material selection decisions for mercury pumps. The performance of nine different alloys – in the as-cast condition as well as following a case-hardening treatment intended to increase surface hardness – was compared in terms of weight loss and surface profile development as a function of sonication time in mercury at ambient temperature. The results indicated that among several potentially suitable alloys, CD3MWCuN perhaps exhibited the best overall resistance to cavitation in both the as-cast and surface treated conditions while the cast irons examined were found unsuitable for service of this type. However, other factors, including cost, availability, and vendor schedules may influence a material selection among the suitable alloys for mercury pumps.

1. INTRODUCTION

The Spallation Neutron Source (SNS) will generate neutrons via interaction of a pulsed proton beam with a liquid mercury target. In order to provide the required cooling and maintain the target temperature within limits, the mercury is pumped through the target module and passed through heat exchangers in a continuous loop. Due to the potential for significant heat generation at/near the target window (point at which the beam directly interacts with the mercury), the mercury pump must be reliable and efficient in order to maintain the desired target temperature profile.

The mercury pump presently in service was fabricated primarily from type 304/316 stainless steel components, including a cast stainless steel impeller. While this material is expected to provide adequate service, it is known from studies of cavitation in mercury that standard grades of stainless steel are somewhat susceptible to erosion damage in mercury when cavitation conditions exist within the fluid.[1, 2] In anticipation of the eventual need for a replacement pump for the mercury loop and a potential power upgrade for the target, screening tests of the relative cavitation-erosion resistance of candidate impeller materials were undertaken to support alternate material selection decisions.

Nine different cast materials were included in the test matrix reported here, selected primarily as a result of informal correspondence with pump manufacturers regarding materials that have been used successfully for pumping mercury and/or were readily available as impellers. In addition to evaluation of the individual materials in the as-cast condition, specimens of each were also evaluated following treatment with a proprietary low temperature carburizing treatment termed Kolsterising® (registered trademark of the Bodycote Company, Apeldoorn, Netherlands) which is known to provide significant surface hardening for materials receptive to the required surface cleaning and carbon doping. In a few cases, the base materials Kolsterised® for this evaluation fall outside the nominal range of compositions that might be routinely considered for this treatment, but nevertheless were treated for this study in an attempt to examine the efficacy of the treatment on new/different materials.

2. EXPERIMENTAL

Cavitation-erosion tests were performed using a titanium vibratory horn and the general test methodology described in ASTM G-32.[3] Each test button (described in detail previously)[1] had a surface area of 180 mm^2 exposed to cavitation conditions and was attached to the horn via a threaded shank. In all cases, the horn tip oscillated at a fixed frequency of 20 kHz and was set to generate a peak-to-peak vibrational amplitude of 25 μm. All tests were conducted in a jacketed stainless steel container, which permitted temperature control via circulation of a water/glycol mixture from a constant temperature bath. The mercury temperature was monitored in the test bath and was maintained at 25-27°C for all tests. The test specimen surface was immersed approximately 2 mm below the surface of the mercury in the center of the container for most tests, but comparison data was also collected for immersion to a depth of 25 mm in some cases. Approximately one liter of high purity mercury was contained within the jacketed vessel and the same mercury was used for all tests. Periodically, cheesecloth was used to skim the mercury surface and remove floating oxides and/or test debris.

Following sonication, test specimens were ultrasonically cleaned sequentially in (1) an aqueous solution containing dissolved thiosulfates and other species to chemically bind mercury, (2) distilled water, and (3) acetone, followed by forced air drying in each case. Specimens were then weighed and examined with an optical microscope to assess the average cavitation-erosion surface profile and to evaluate pitting. The profile determination was performed with the calibrated fine focus feature of the optical microscope. Each division on the fine focus knob corresponds to a one-micron vertical movement of the microscope stage, so by sequentially focusing first on the relative high point and then on the low point within a field of view, the depth of surface relief can be estimated. Typically, the average profile was determined from measurements at 400x on seven random but regularly spaced locations across the test surface, with observations of areas of profile significantly different than the average noted as appropriate.

Following sonication, selected specimens were also sectioned for metallographic assessment of the profile and microstructural effects at the specimen surface. Post-test specimens were cut and mounted in cross-section to reveal the test surface as well as the specimen edges and threaded region. Standard mounting and polishing techniques were employed and the cross-sections were examined in both the as-polished and etched conditions.

Microhardness scans were made on selected cross-sections in the as-polished condition. The near-surface hardness was determined via diamond indenter with a 50-g load (25-g load in a few limited cases), and hardness profiles across any hardened regions were performed by advancing across the surface layer at an angle to permit multiple hardness indentions to be made within very thin surface layers without being too close to an adjacent indentation. While hardness measured in this way may have limited utility in an absolute quantitative sense, the relative hardness across thin layers can be readily compared to the substrate hardness.

Nine cast materials were evaluated in this study. In each case, test buttons were machined from as-cast material obtained from a variety of suppliers/sources. Subsequently, the test face of each specimen was abraded on 800 grit silica paper to ensure a uniform starting surface condition among all specimens. Specimens of each material (as-cast, machined, 800-grit finish on test face) were also subjected to the Kolsterising® treatment. Depending on the specific alloy composition, specimens received either the “duplex” process or the “standard” process to carburize the materials. The “duplex” process imposes conditions that lead to a case depth of about 18 μm in type 316 stainless steel, and this treatment was applied to the CD3MWCuN and CD3MN alloys studied here. All other alloys treated for this study received the “standard” process, which imposes conditions leading to a case depth of about 38 um in type 316 stainless steel. For comparison, equivalent specimens representing wrought 316LN stainless steel in the annealed condition were also included within the test matrix. A summary of material composition and related information is given in Table 1.

To interpret the test results, it is important to recognize that there is no known direct correlation between the damage rate/intensity produced at the tip of the vibratory horn and potential cavitation damage on an impeller pumping mercury. The tests performed here simply represent a comparative screening evaluation among materials exposed to a fixed set of test conditions, which are expected to offer an aggressive and perhaps accelerated assessment of potential cavitation-erosion damage. In this fashion, relative cavitation-erosion performance can be compared and eventually interpreted in terms of other advantages/disadvantages of each candidate material.

Table 1. Composition and related information for the alloys investigated. Composition of all alloys from certified mill reports except for HC-600 for which the nominal composition is given.

Cast alloy	**CA-15**	**CF8M**	**CW12MW**	**CD3MWCuN**	**CD3MN**
(Wrought equivalent)	410 stainless	316 stainless	Alloy C	Xeron 100	2205 stainless
Structure [a]	Mostly martensitic	Duplex (~10 δ)	Wholly austenitic	Duplex (~50 δ)	Duplex (~70 δ)
Bulk hardness[b]	R_c = 43	R_b = 86	R_b = 91	R_c = 23	R_c = 20
Treatment condition	As-cast	As-cast	As-cast	As-cast	As-cast
Element (wt %)					
C	0.12	0.05	0.03	0.03	0.03
Mn	0.31	0.77	0.75	0.28	0.65
P	0.012	0.021	0.006	0.022	0.025
S	0.006	0.027	0.003	0.008	0.006
Si	1.02	1.26	0.7	0.8	0.71
Fe	Balance	Balance	5.5	Balance	Balance
Cr	12.3	19.3	16.0	25.3	22.6
Ni	0.51	9.9	balance	8.0	4.9
Mo	0.01	2.41	16.5	3.7	3.0
N				0.29	0.18
Cu				0.86	0.89
W			4.0	0.59	
V			0.25		

Table 1. (Cont'd)

Cast alloy	Grey cast iron (Class 30)	Grey cast iron (Class 40)	Ni-resist	HC-600	
(Wrought equivalent)					316LN
Structure	Pearlite+ Graphite	Pearlite+ Graphite	Wholly Autsenite	Martensite +Austenite	Wholly Austenite
Bulk hardness	R_b = 86	R_b = 91	R_b = 75	R_c = 58	R_b = 55
Treatment condition	As-cast	As-cast	As-cast	As-cast + hardened	Annealed
Element (wt%)					
C	3.190	3.310	2.920	2.0-3.3	0.009
Mn	0.644	0.740	1.140	2.0 max	1.75
P	0.071	0.107	0.186	0.1 max	0.029
S	0.056	0.057	0.030	0.06 max	0.002
Si	2.664	2.610	2.440	1.5 max	0.39
Fe	Balance	Balance	Balance	Balance	Balance
Cr			2.20	23-30	16.31
Ni			14.09	2.5 max	10.20
Mo				3.0 max	2.07
N					0.11
Cu			6.10	1.2 max	0.23
W					
V					

[a]Structure symbol for ferrite is δ; remainder of duplex structure is austenite unless otherwise indicated.
[b]Based on bulk surface measurements in on as-received material.

3. RESULTS AND DISCUSSION

3.1 GENERAL TRENDS AND COMPARISONS

Recent cavitation testing of stainless steel in mercury with a vibratory horn indicated potential sensitivity of the results to test configuration. In particular, variations in bath volume and/or immersion depth of the specimen test face seemed to influence the results quantitatively, but with no change in the general trends.[4] In an attempt to examine immersion depth as a potential test variable, vibratory horn test results for the as-received (no surface treatment) cast materials and the wrought/annealed 316LN were compared at immersion depths of 2 mm and 25 mm, with all other test variables remaining constant. For each material, duplicate exposures of 3 h in length were performed for each immersion depth. The overall results are summarized in Table 2. Results for identical specimens were found to be very reproducible – within a few percent – for consistent test conditions; details for individual alloys appear in Section 3.2.

The data in Table 2 reveal that in every case for which a comparison was attempted, the average surface profile following a 3 h exposure was greater for the 2 mm immersion depth condition. In some cases, particularly when resistance to cavitation-erosion is relatively high, the difference is small but nevertheless reproducible. Only 5 of 8 materials exhibited a corresponding increase in weight loss for the 2 mm immersion condition, but the average increase among those five was almost 30%. [Note that while weight loss and surface profile tend to be related, it must be recognized that the development of surface profile includes relatively uniform material removal as well as physical deformation which is sometimes quite localized. As a result, it is possible for a specimen to exhibit high weight loss and low surface profile development or vice versa.] While these results suggest that the 2 mm immersion condition is at least somewhat more aggressive than the 25 mm immersion condition, the relative ranking of these materials is essentially independent of the immersion depth variable in these tests. However, as a result of the indication that 2 mm immersion is somewhat more aggressive, this condition was used to evaluate the limited number of Kolsterised® specimens included in the test matrix.

Table 2. Comparison of average cumulative weight loss and average surface profile for untreated (not Kolsterised®) specimens sonicated for three total hours in mercury at 25-27°C. Two identical specimens exposed for each immersion condition. Abbreviation GCI represents gray cast iron.

	2 mm immersion depth		25 mm immersion depth		% change[a]	
Material	**Wt loss (mg)**	**Profile (µm)**	**Wt loss (mg)**	**Profile (µm)**	**Wt loss**	**Profile (µm)**
CD3MWCuN	5.38	12	5.58	11.5	-4	+4
HC-600	4.71	16	6.17	15	-24	+7
CA-15	6.59	18	5.35	17.5	+23	+6
CD3MN	10.77	19	8.47	14	+27	+36
CW12MW	9.30	25	7.92	22	+17	+14
CF8M	15.51	28	11.54	21	+4	+33
316LN	29.73	51	22.23	44	+34	+16
GCI-Class 40	49.77	80	[b]	[b]		
CGI-Class 30	63.11	121	69.87	102	-10	+19
Ni-resist	99.82	152	[b]	[b]		

[a]% change calculated as [(2 mm result) – (25 mm result)]/(25 mm result) for the total weight change or profile development observed at the end of 3 h sonication. Change based on slopes of weight change curves are discussed in a subsequent section.

[b]No test for this condition.

The materials in Table 2 are listed from most resistant (top) to least resistant (bottom) to cavitation-erosion in mercury. In some cases, the relative resistance among materials is very similar, but when relative weight loss among materials was a poor discriminator, profile development was used to distinguish relative ranking/performance (and vice versa). As an example, CD3MWCuN is ranked as slightly superior to HC-600, despite a 14% lower weight loss for HC-600 in the 2 mm immersion. However, the surface profile of the CD3MWCuN was lower by 25%, and was not prone to isolated pitting as was the HC-600. Further, the CD3MWCuN was more generally corrosion resistant, as exhibited by less aggressive wetting of mercury and no staining/discoloration during the cleaning process. The relative ranking between these two materials is more straightforward for the 25 mm immersion condition.

The relative cavitation-erosion resistance of the as-cast alloys (reproduced from Table 2) is reordered as a function of the material hardness in Table 3. Note that while increased hardness is often considered a bellwether of improved cavitation-

erosion resistance, Table 3 indicates several exceptions to such a rule-of-thumb. For example, while the hardest materials are all among the materials yielding the least weight loss and profile development, perhaps the best overall material (R_c 23) is considerably softer than the hardest material (R_c 58). Further, two different materials with the same hardness (R_b 91) exhibited very different cavitation-erosion behavior in mercury. [Another pair of materials with hardness R_b 86 revealed similarly diverse cavitation-erosion results.] Finally, consider that the softest material tested (R_b 60) reveals superior cavitation-erosion resistance to at least three somewhat harder materials. The point here is not that the relative hardness generality has no merit, but that cavitation-erosion resistance is clearly a function of composition and structure as well as hardness.

Table 3. Untreated test materials ranked in order of macro-hardness along with the cavitation-erosion data for three hour exposures (2 mm immersion depth). Hardness values in the table decrease from top to bottom; for comparison between hardness scales, note that R_b 91 is approximately equal to R_c 10.

As-cast material	Hardness	Wt loss (mg)	Profile (µm)
HC-600	R_c = 58	4.71	16
CA-15	R_c = 43	6.59	18
CD3MWCuN	R_c = 23	5.38	12
CD3MN	R_c = 20	10.77	19
CW12MW	R_b = 91	9.30	25
GCI-Class 40	R_b = 91	49.77	80
CF8M	R_b = 86	15.51	28
CGI-Class 30	R_b = 86	63.11	121
Ni-resist	R_b = 75	99.82	152
316LN[a]	R_b = 60	29.73	51

[a]Wrought/annealed 316LN included for comparison with cast materials.

Cavitation-erosion data was also collected for specimens treated with the Kolsterising® process for the 2 mm immersion condition. Weight loss and surface profile results are summarized in Table 4, and Table 5 compares weight loss and profile as a ratio of results for the untreated and treated specimens for each material. In summary, these results suggest that the Kolsterising® process significantly improved (by a factor of two or more on weight loss or profile or both) the cavitation-erosion resistance

of the cast materials CD3MN, CD3MWCuN, CF8M, and CW12MW. Since the primary mechanism of improvement associated with the Kolsterising® process is surface hardening via carburization, it is not surprising that the two hardest materials, HC-600 and CA-15, each improved only marginally as a result of the Kolsterising® treatment. The cavitation-erosion resistance of the two gray cast irons and the Ni-resist material was degraded by the Kolstersing® treatment as evidenced by even higher weight losses and more rapid profile development compared to the untreated specimens.

It is interesting that the greatest improvement in cavitation-erosion resistance as a result of Kolsterising® was observed for the wrought/annealed 316LN included in the data sets here to facilitate ready comparison of the results for the cast materials with extensive previous data for wrought alloys with different treatments.[1, 2] In part, the superior response of the 316LN is due to the very low hardness of the base material – it therefore stands the most to gain from a surface hardening process. However, the fact that 316LN is an iron base alloy with modest chromium and nickel content in an austenite crystal structure makes it ideally suited to low temperature carburization yielding maximum hardening without substantial formation of deleterious phases. [See Farrell, et al.,[5] for extensive documentation of the Kolsterised® surface layer on 316LN stainless steel.] CF8M and CD3MN, both duplex materials, contain significant fractions of austenite with similar composition to that in the wrought 316LN, and therefore it seems reasonable that these alloys would exhibit the greatest improvements among the cast alloys following the Kolsterisation® treatment.

3.2 RESULTS FOR INDIVIDUAL ALLOYS

3.2.1 CF8M

CF8M is considered the cast equivalent of 316 stainless steel and in general these alloys exhibit remarkably similar bulk composition. The primary difference between the cast and wrought grades are that the latter has a wholly austenitic structure with a small and uniform grain size, while the former typically exhibits a small amount of residual ferrite in the large-grained austenite that results from the casting process. Due primarily to the very similar composition, type 316 and CF8M are nominally specified for use in many of the same chemical environments.

Table 4. Average cumulative weight loss and average surface profile for Kolsterised® specimens sonicated at 2 mm immersion depth for a total of three hours in mercury at 25-27°C. Two identical specimens exposed for each material. Abbreviation GCI represents gray cast iron.

Kolsterised® material	Wt loss (mg)	Average surface profile (µm)	Observations
CD3MN	2.22	5	No pitting
CD3MWCuN	2.34	8	Few shallow, widely scattered pits
316LN [a]	2.53	5	Few shallow, widely scattered pits
CF8M	3.34	13	Few shallow, widely scattered pits
CW12MW	3.57	18	Dense pitting
CA-15	3.83	15	Dense pitting
HC-600	4.19	15	Dense pitting, non-uniform discoloration
GCI-Class 40 [b]	44.6	75	Dense cratering and discoloration
CGI-Class 30 [b]	54.5	142	Dense cratering and discoloration
Ni-resist [b]	71.1	169	Extensive cratering and ~disintegration

[a] Wrought alloy; included here for comparison.
[b]T tested only two hours; results significantly inferior to results for untreated specimens.

Table 5. Comparison of cavitation-erosion performance for treated and untreated cast alloys. Calculation ratio based on average of two specimens sonicated three hours each in mercury at 2 mm immersion depth, except for materials denoted “a” which are for specimens sonicated similarly for two hours. Data for wrought annealed 316LN included for comparison.

Kolsterised® material	Wt loss results; ratio of untreated/treated	Profile results; ratio of untreated/treated
CD3MN	4.9	3.8
CD3MWCuN	2.3	1.5
316LN	11.8	10.2
CF8M	4.6	2.2
CW12MW	2.6	1.4
CA-15	1.7	1.2
HC-600	1.1	1.0
GCI-Class 40	0.7	0.9
CGI-Class 30	0.8	0.6
Ni-resist	0.8	0.8

Figure 1 summarizes the cavitation-erosion data collected for this alloy in the present study. After an initial incubation period – that is, the sonication time necessary to initiate and coalesce microcracks sufficiently large to effect detectable material removal from the surface – the slope of the weight loss curves is essentially constant, even to the extended exposure time of 6 h, for each type of specimen and test condition. Consistent with the trend indicated in Table 2, Fig. 1 shows that the 2 mm immersion depth (weight loss rate about 6.8 mg/h) in mercury is a significantly more aggressive test condition that the 25 mm immersion depth (~4.6 mg/h) for the untreated material. The treated specimens yielded a mass loss rate of about 0.8 mg/h (2 mm depth) – essentially identical to the value observed for successfully Kolsterised® surfaces of 316LN which routinely falls in the range 0.7-0.8 mg/h.[2]

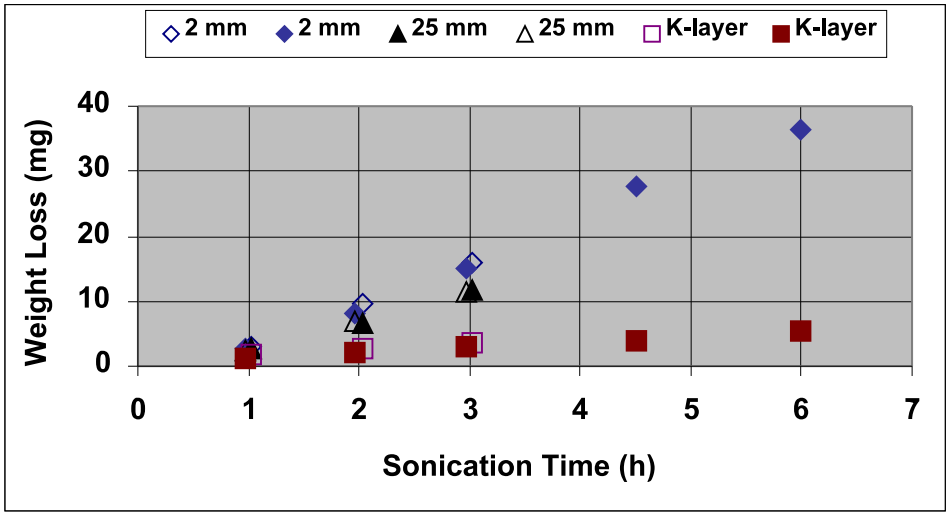

Fig. 1. Weight loss as a function of sonication time in Hg for untreated specimens (2 mm and 25 mm immersion depth) and treated specimens (2 mm immersion depth) of as-cast CF8M. Note that data points are sufficiently close together that several are at lest partially obscured. "K-layer" designation indicates specimens treated with the Kolsterisation® process. The treated specimens exhibit much reduced weight loss.

Figure 2 is a macrograph of the untreated CF8M test surface following 6 h sonication (2 mm depth) in mercury. Considerable surface relief and a few pits/craters are obvious, but note that the surface relief is not uniform across the specimen surface but rather seems to be sensitive to the particular grain orientation exposed to the test surface. Using the microscope to estimate relative surface profile indicated some areas (whole grains) revealed as little as 35-40 μm of profile following 6 h exposure, but

adjacent grains exhibited as much as 100 μm of profile and individual pits 150 μm or more deep.

Fig. 2. Test surface of an untreated CF8M test button (actual diameter = 16 mm) following 6 h sonication (2 mm depth) in mercury. Surface relief appears related to grain orientation.

Figure 3 shows a cross section of the untreated CF8M test surface following sonication for 6 h (2 mm depth) and, in this particular area, it reveals typical surface roughening (about 30 μm that includes some general surface ablation) as well as a portion of an individual pit. The discontinuous second phase comprising about 10% of the material is the ferrite phase, and Fig. 3 also shows that it was eroded at a rate indistinguishable from that of the austenite. Also note, in the highest magnification view, the roughness at the bottom of the pit shows the non-uniform advance of the eroding interface. In other grains, the general pitting was somewhat deeper but otherwise identical to the appearance in Fig. 3.

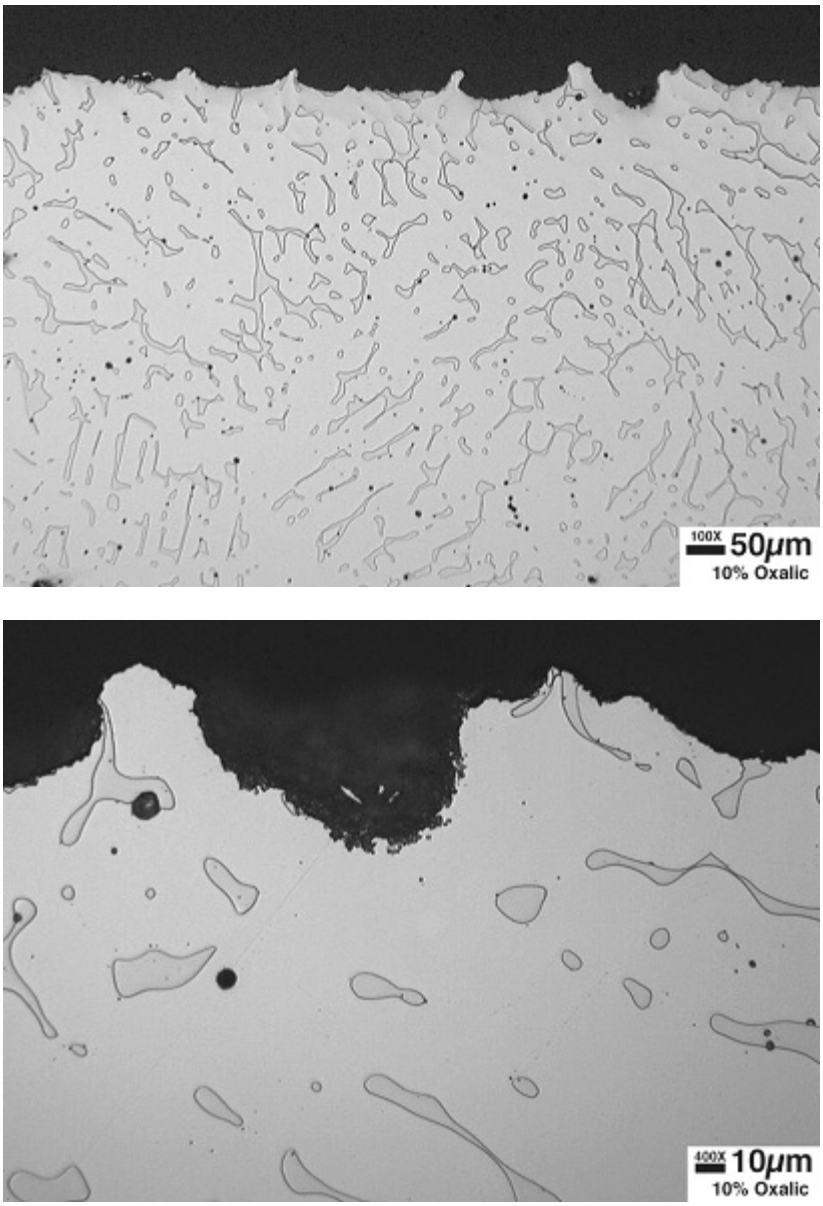

Fig. 3. Etched cross section of the untreated as-cast CF8M specimen following sonication (2 mm depth) in mercury for six hours. In both views (representing the same general area, higher magnification at bottom), the specimen surface meets the black mounting epoxy near the top of the photograph.

The thickness of the Kolsterised® layer on the treated specimens was particularly difficult to distinguish via the chemical etching required to reveal the general microstructure of this specimen, but adjustment of the focus and microscope lighting suggested a relatively uniform layer 10-12 μm thick remaining on the test surface. The

test surface also exhibited scattered surface roughness approximately the same depth, indicating breaching of the protective layer in localized areas of the exposed surface. Microhardness scans confirmed a remaining layer of about 12-15 μm of hardened (compared to the as-received value) material on the test surface, and measurements on unexposed (edges, threads) portions of the test button indicated that the as-treated depth of the hardened layer was approximately 20 μm, with a maximum hardness near R_c 53.

Figure 4 compares scanning electron microscope (SEM) photographs of the test surface of a treated and an untreated CF8M specimen following sonication in mercury for six hours (2 mm depth). These photographs reveal that the untreated specimen readily developed typical surface roughness and pits/craters associated with specimens sonicated in mercury with the vibratory horn[1, 2] while the treated specimen is considerably more resistant (but not entirely immune) to these manifestations of cavitation-erosion. In particular, note that the general roughness characteristics are similar for both the treated and untreated specimens, but the softer untreated surface apparently yields much more readily to the bombardment of mercury cavitation.

3.2.2 CD3MWCuN

The most highly alloyed stainless steel evaluated in the present investigation, this duplex cast stainless steel has a composition and mechanical properties covered by ASTM A890. As a generality, this alloy exhibits good aqueous corrosion resistance in a wide range of aggressive environments and its duplex structure tends to render it particularly resistant to environmentally induced cracking.

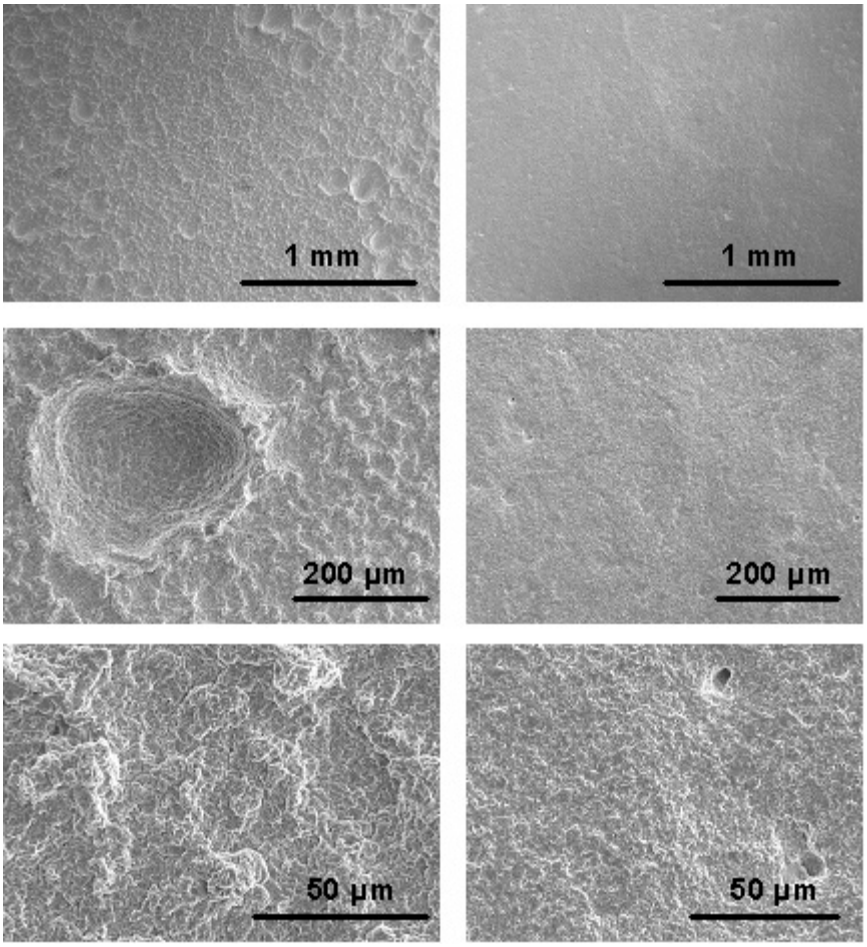

Fig. 4. SEM photographs of untreated (left column) and treated (right column) as-cast CF8M following six hours sonication in mercury (2 mm depth). Magnification increases by a factor of 20 from the top photo to the bottom photo. Observe that the treated material was much more resistant to cavitation-induced surface damage than the untreated material.

Figure 5 summarizes the cavitation-erosion data gathered for CD3MWCuN during this evaluation. The data reveals that the performance of the untreated specimens, whether immersed 2 mm or 25 mm in mercury, is indistinguishable (also noted in Table 2), and the slope of the weight loss curves for the untreated materials is essentially constant at about 2.0 mg/h, even to the extended exposure time of 6 h for one untreated specimen. Figure 6 shows the untreated test specimen surface following the 6 h exposure – note the relatively smooth and pit-free surface. Post-test metallography of this specimen confirmed only a very modest roughness of up to 15 µm, and that the ferrite and austenite phases were similarly eroded (that is, neither was attacked preferentially).

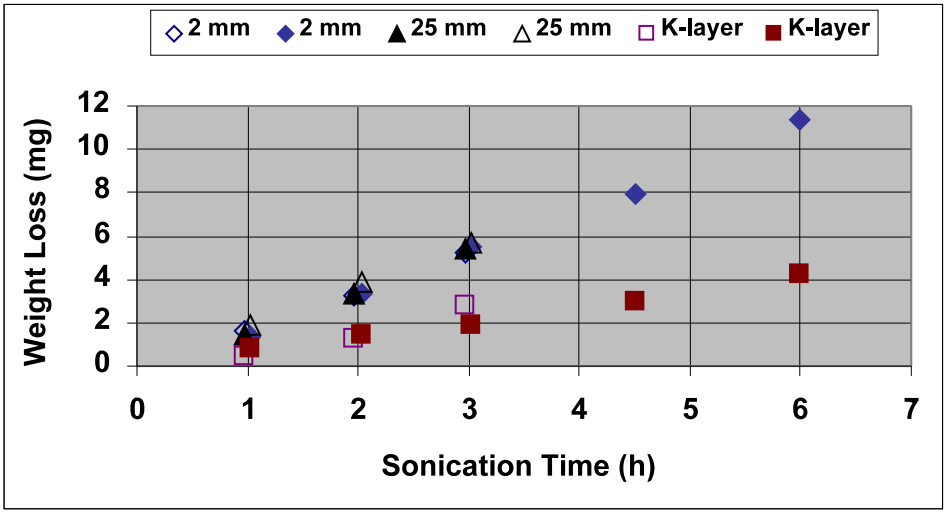

Fig. 5. Weight loss as a function of sonication time in mercury for untreated specimens (2 mm and 25 mm immersion depth) and treated specimens (2 mm immersion depth) of as-cast CD3MWCuN. "K-layer" indicates specimens treated with the Kolsterisation® process. Note that data points are sufficiently close together that several are at least partially obscured.

Fig. 6. As-received CD3MWCuN specimen (actual diameter = 16 mm) following sonication for 6 h (2 mm depth) in Hg. Note the relatively smooth and pit-free surface.

Following the incubation period, the slope of the weight loss curves for the treated specimens (Fig. 5) is approximately constant at 0.7 mg/h, or about a third the value of the untreated specimen. As noted previously, this value is similar to that observed for 316LN wrought material and several other successfully treated specimens.

Macroscopically, the treated test surface was essentially smooth and featureless following 6 h sonication. Figure 7 shows the cross section of the treated specimen surface following 6 h exposure – note the almost completely smooth surface (average profile only about 5 μm) with no pitting. The austenite phase, which is the rounded and secondary/discontinuous constituent in the structure, reveals a band of material about 10 μm wide at the exposed surface that is full of slip lines but otherwise featureless. This is the hardened material resulting from the carburization process. The ferrite phase, which has a different crystal structure and composition, has much less solid solubility for carbon than austenite and therefore does not exhibit the same type of reaction layer. Rather, the density of chromium carbides in the near-surface ferrite is very high resulting from reaction with the carburizing environment (and revealed by heavier etching than that shown in Fig. 7) but no uniform reaction layer analogous to that in the austenite can be readily discerned.

Although the reaction layer in the austenite is too thin for precise measurements of a hardening profile, micro-hardness measurements indicate that the center of the case depth in austenite exhibits a hardness of about R_c 36-37, suggesting that a value somewhat higher exists on the test surface proper. The hardness of the austenite decreases rapidly with distance from the treated surface, but some modest hardening persists for 40 μm or so, which probably results from a combination of carbon diffusion into the material and local work hardening of the surface as a result of the bombardment associated with the cavitation process.

Figure 8 compares SEM photographs of the surface of untreated and treated specimens of CD3MWCuN following 6 h sonication experiments. The untreated specimen is only slightly rougher in surface profile, consistent with about a factor of 2-3 greater total weight loss for the untreated specimen over the short exposure period.

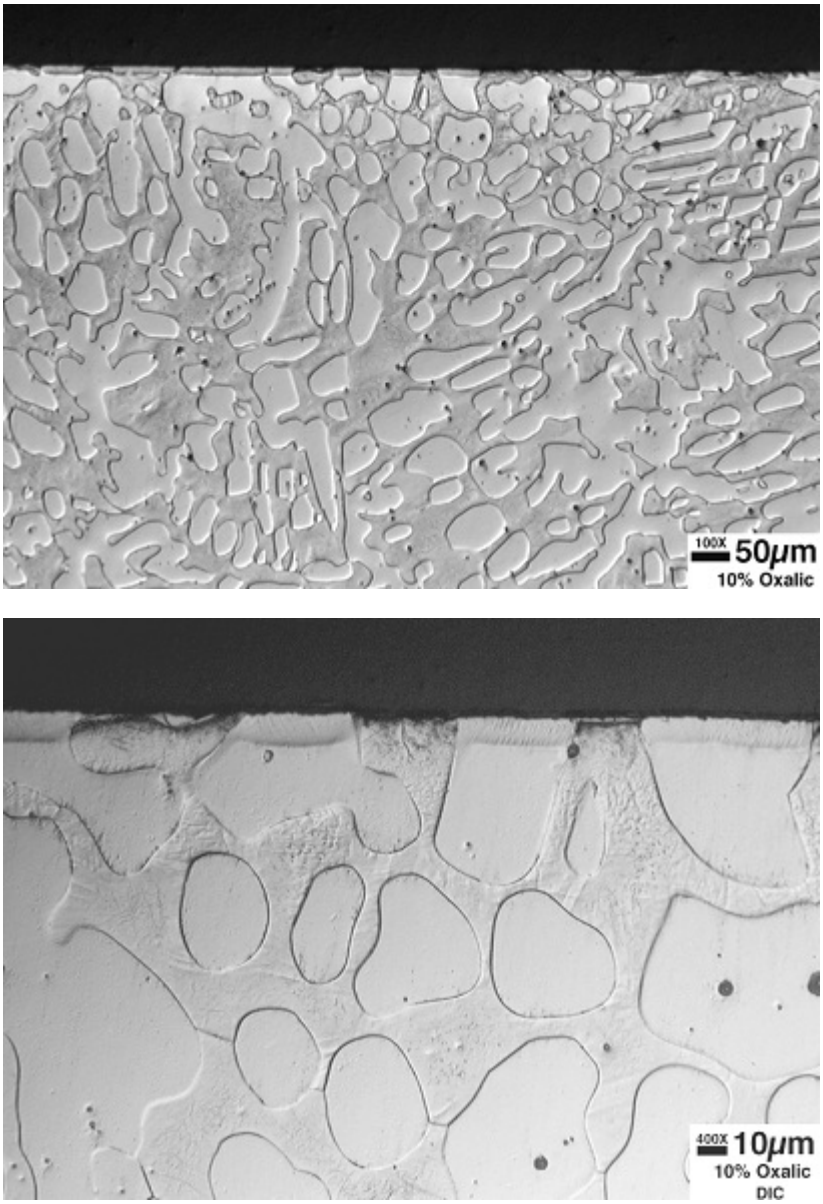

Fig. 7. Cross section of treated CD3MWCuN specimen following sonication in mercury for 6 h. In both views (representing the same general area, higher magnification at bottom), the specimen surface meets the black mounting epoxy near the top of the photograph. Specimen surface appears smooth and free of pits.

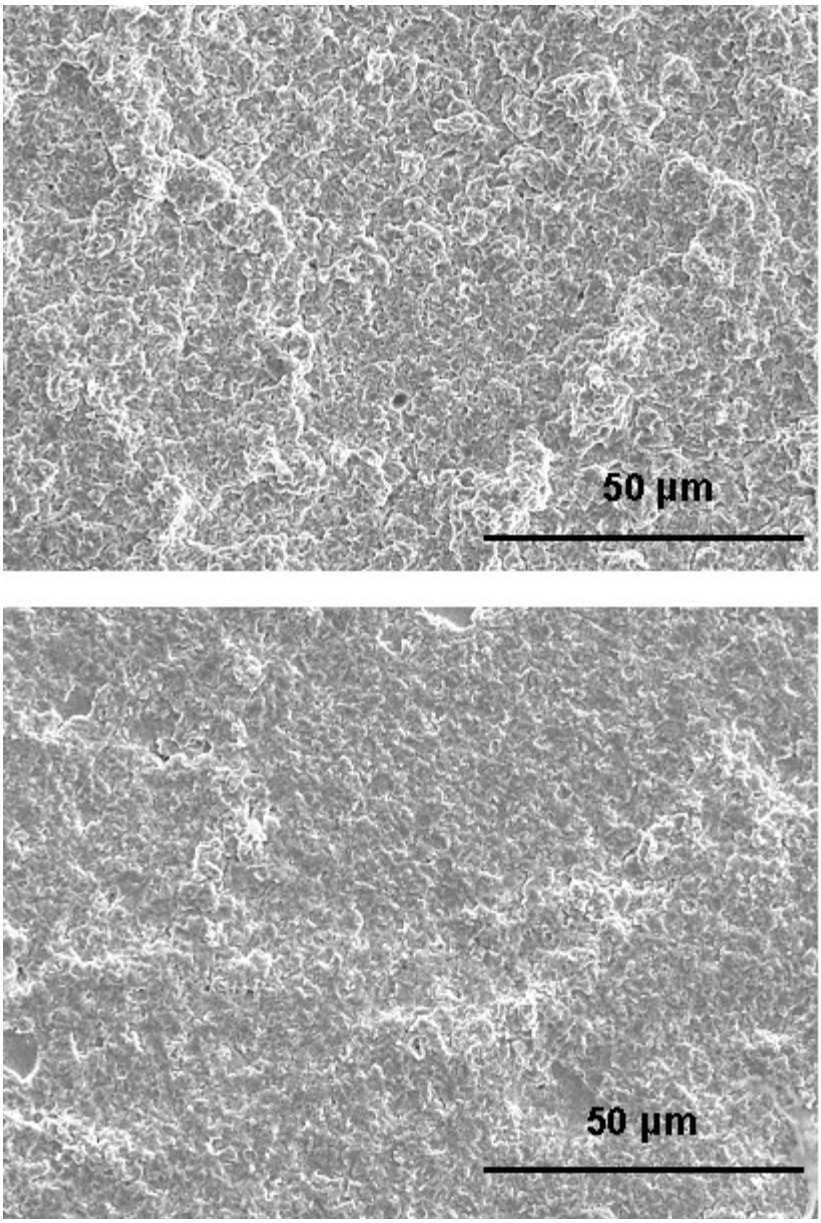

Fig. 8. SEM photographs of the untreated (top) and treated (bottom) CD3MWCuN specimens following 6 h sonication in mercury. The untreated surface is only slightly rougher than the untreated surface.

3.2.3 CA-15

CA-15 is a martensitic stainless steel usually specified for cases requiring only modest corrosion resistance but with somewhat elevated mechanical property requirements compared to other common stainless steels. The relatively low chromium content of this alloy renders it susceptible to corrosion in environments readily resisted by more highly alloyed “stainless” materials.

Figure 9 shows the weight loss data as a function of sonication time for the CA-15 specimens. Although there was more scatter in the data for CA-15 than several other materials, it is apparent that the weight loss rate was somewhat greater for the 2 mm depth test condition (~2.5 mg/h) than for the 25 mm depth test condition (~1.9 mg/h).

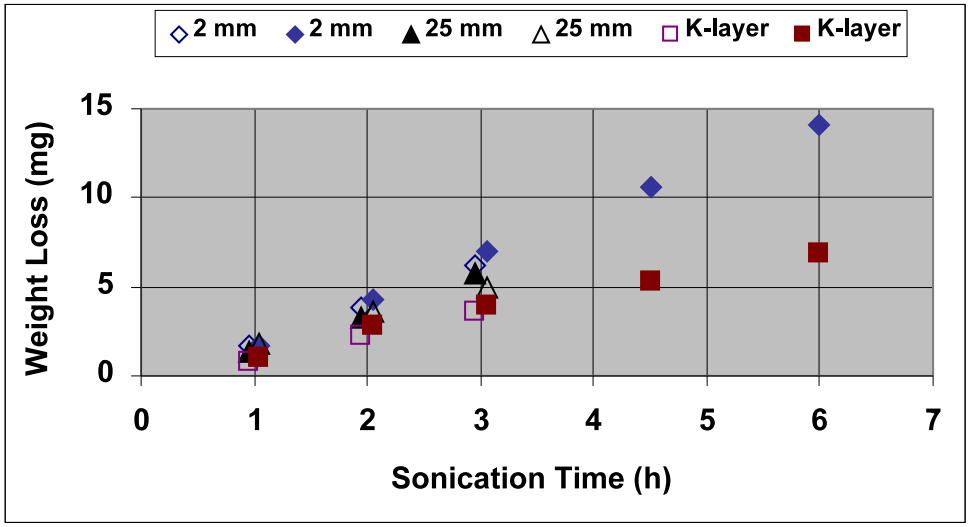

Fig. 9. Weight loss as a function of sonication time in mercury for untreated specimens (2 mm and 25 mm immersion depth) and treated specimens (2 mm immersion depth) of as-cast CA-15. "K-layer" indicates specimens treated with the Kolsterisation® process. Note that data points are sufficiently close together that several are at least partially obscured.

Figure 10 is a macrograph of the CA-15 test specimen sonicated 6 h in mercury at the 2 mm immersion depth. Compared to the other "stainless" alloys in this investigation, the CA-15 specimens were significantly discolored following exposure, but the aqueous cleaning procedure contributes somewhat to this behavior. The test surface reveals a general roughening and a number of modest pits generally in the range of 75-100 μm deep.

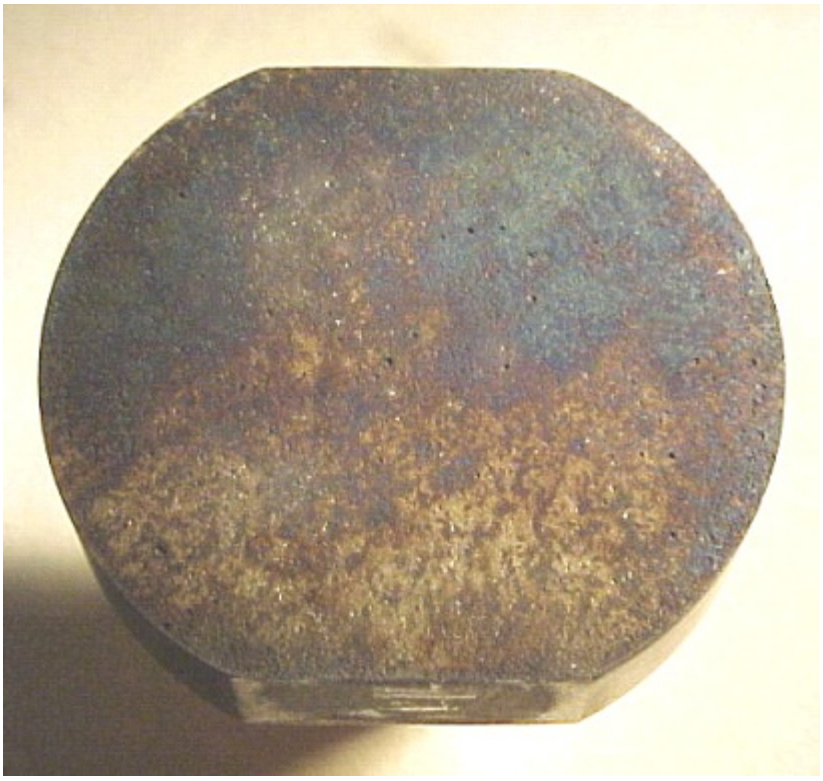

Fig. 10. As-received/untreated CA-15 specimen (actual diameter = 16 mm) following sonication for 6 h (2 mm depth) in mercury. Note significant discoloration and pits scattered across the surface.

Figure 11 shows a representative cross section of the specimen shown in Fig. 10. These views confirm only a modest general roughness (approximately 15-20 μm) and a number of pit embryos that are somewhat different than the nominal hemispherical shape. Although insufficient data was collected to state with certainty, there is some microstructural evidence that these small pits initiate at areas where the residual ferrite (ringed with hard but brittle carbides) in the martensitic matrix intersects the specimen surface. In particular, note the pit/crater shapes in the middle and bottom photos of Fig. 11 showing residual ferrite exclusively at the bottom of the pit.

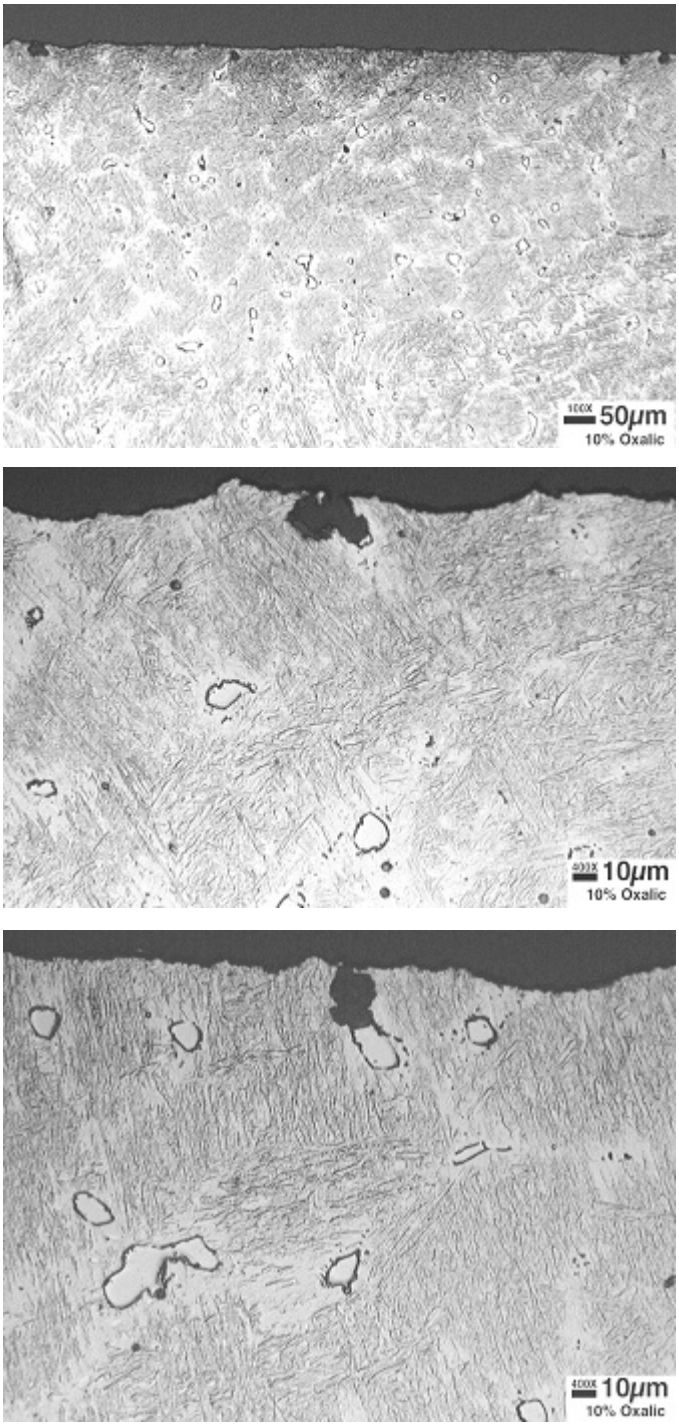

Fig. 11. Cross section of untreated CA-15 specimen following sonication in mercury for 6 h. In all views (representing the same general area, higher magnification photos at bottom), the specimen surface meets the black mounting epoxy near the top of the photograph. Photograph at the bottom reveals residual ferrite at the bottom of the pit.

The Kolsterising® treatment produced a relatively small improvement in cavitation-erosion performance compared to the untreated specimens. Based on total weight loss and slope of the weight loss curves, an improvement factor of only about two was observed. Of particular note was the slope of the weight loss curves for the treated specimens – about 1.0 mg/h – which is a modest but significant increase compared to the 0.7-0.8 mg/h rate exhibited by many other alloys with a Kolsterised® surface.

Figure 12 shows the treated CA-15 specimen following 6 h sonication time (2 mm depth), which reveals widespread discoloration of the test surface. Although it is not particularly evident in Fig. 12, the other surfaces of the test specimen (sides, threads) were not similarly discolored. This observation suggests that material exposed and/or left behind on the test surface as a result of the cavitation-erosion process is responsible for the majority of the discoloration.

Fig. 12. Treated CA-15 specimen (actual diameter = 16 mm) following sonication for 6 h (2 mm depth) in mercury. Specimen surface reveals significant discoloration following testing.

Figure 13 is a representative cross section of the specimen shown in Fig. 12. While the general roughness/profile of the treated specimen is very modest (~10-15 μm), there are locations indicating significant penetration – again, perhaps as a result of dislodging ferrite pools intersecting the test surface. [Note the ferrite pool just to the

right of the large penetration in the photograph; it is obviously fractured in the central region, probably as a result of being exposed to the test surface in a nearby cross section.] The total number of these indications is small, but they indicate susceptibility for localized erosion damage that is not present for several other alloys examined.

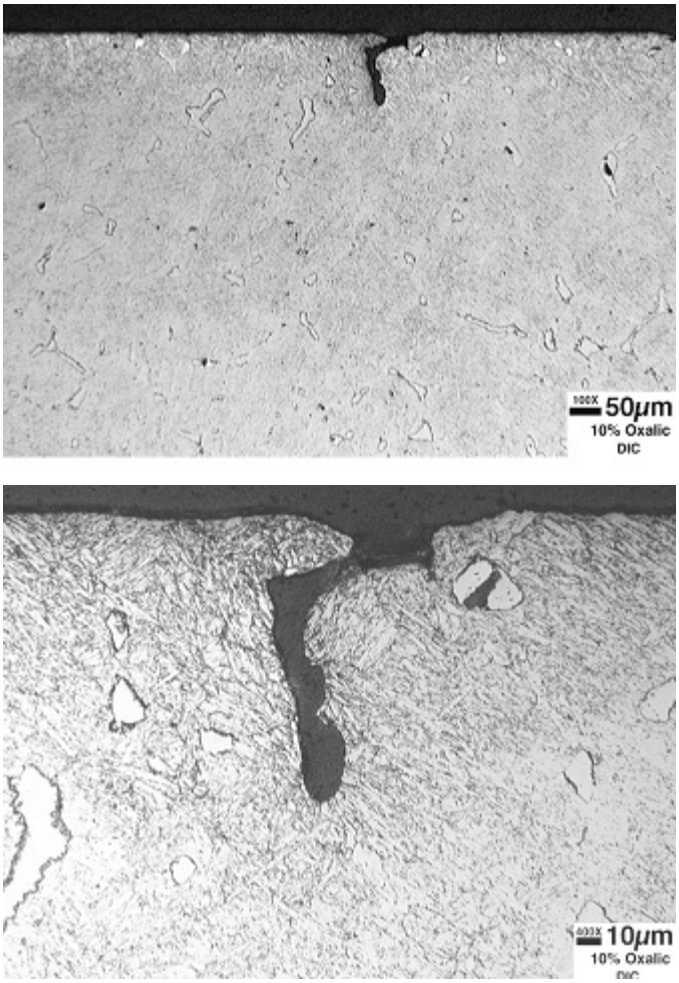

Fig. 13. Cross section of treated CA-15 specimen following sonication in mercury for 6 h. In both views (representing the same area, higher magnification at bottom), the specimen surface meets the black mounting epoxy near the top of the photograph. Note in particular the fracture in the ferrite pool just to the right of the main penetration (former ferrite pool) in the bottom photo.

Figure 14 compares untreated and treated surfaces of as-cast CA-15 following sonication for 6 h in mercury. Note that the treatment process does not eliminate susceptibility to the sharp, angular pitting described above. However, the treatment process does apparently minimize susceptibility to general pitting and profile development, as evidenced by the generally smoother surface of the treated specimen.

The microhardness profiles at the specimen surface indicated a peak hardness of about R_c 62 and a case depth of about 40 μm on both the unexposed areas and the test surface itself. Although an etching procedure to highlight the case hardened region proved elusive for CA-15, a faint hint of a band roughly parallel to the specimen surface about 40-50 μm wide (slightly darker etching; extends about the same depth as the cavitation penetration) was observed.

3.2.4 CD3MN

This is a relatively high alloy, duplex cast stainless steel, with composition and mechanical properties covered by ASTM A890. As a generality, this alloy exhibits good aqueous corrosion resistance and in particular has a reputation for resistance to stress-corrosion cracking in a wide range of aggressive environments.

Figure 15 shows the weight loss data as a function of sonication time for the CD3MN specimens examined in this study. For the untreated specimens, the slopes of the weight change curves reveal that the 2 mm depth exposure (weight loss rate of 4.7 mg/h) was more aggressive than the 25 mm depth exposure (3.3 mg/h) by close to 45%. Figure 16 shows the surface of the untreated specimen following 6 h sonication (2 mm depth) and it reveals general. roughening of the surface (the “wrinkled” appearance of the surface) but no substantial pitting.

Figure 17 shows a representative cross section of the specimen pictured in Fig. 16. The cross section reveals a microstructure with about 30% austenite (light colored discontinuous phase) in a ferrite matrix. Close examination of the test surface suggests that both phases erode at equivalent rates. In this specific location, the general surface roughness is almost 40 μm.

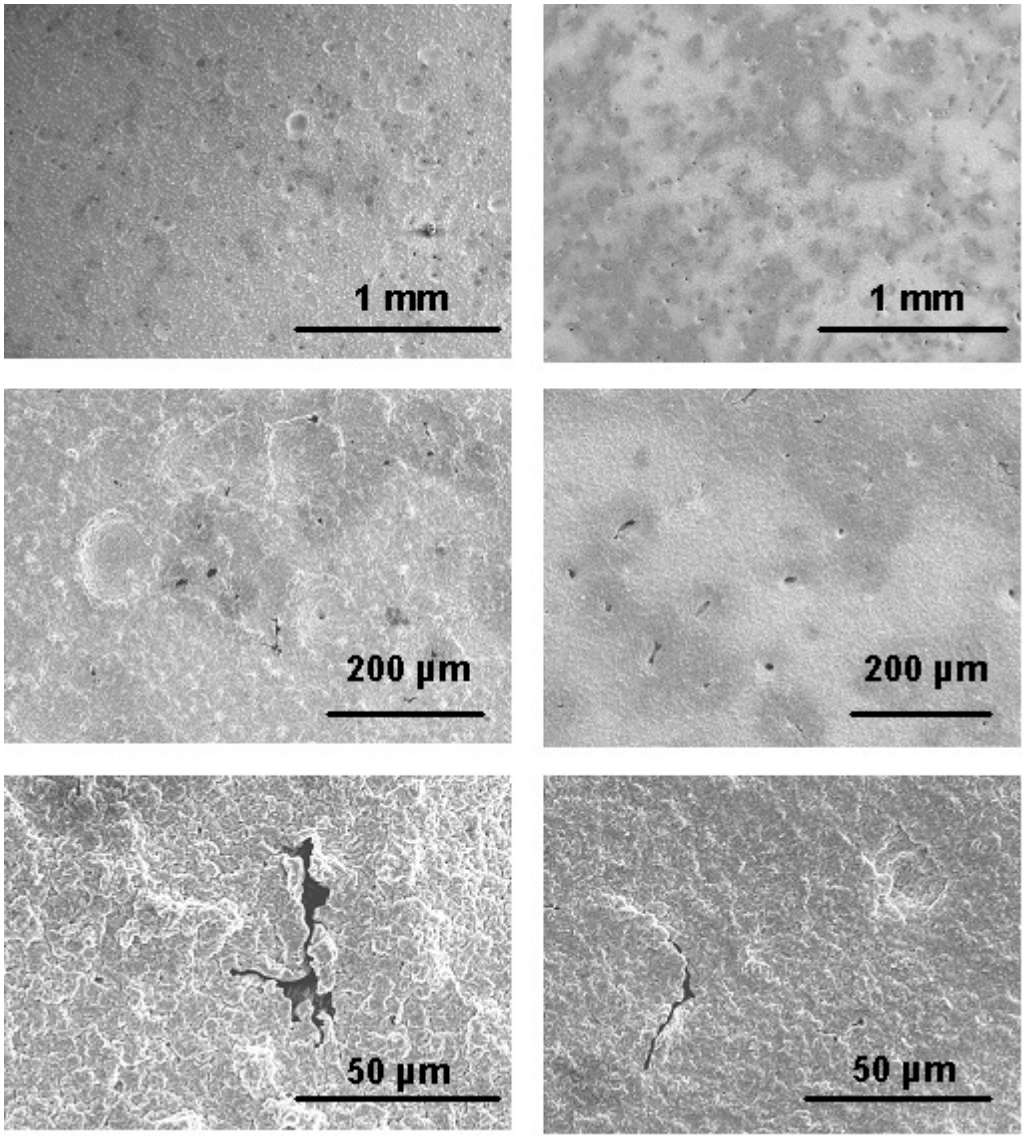

Fig. 14. SEM photographs of untreated (left column) and treated (right column) as-cast CA-15 following six hours sonication in mercury (2 mm depth). Magnification increases a factor of 20 from the top photo to the bottom photo. Note the development of small angular pits is similar for the treated and untreated specimens.

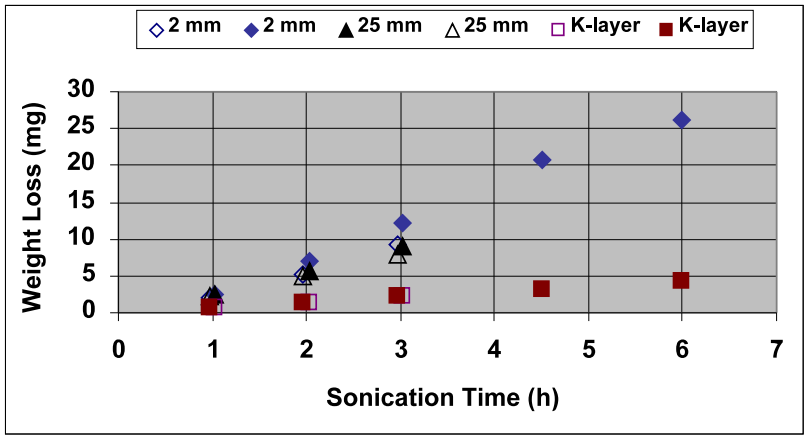

Fig. 15. Weight loss as a function of sonication time in mercury for untreated specimens (2 mm and 25 mm immersion depth) and treated specimens (2 mm immersion depth) of as-cast CD3MN. "K-layer" indicates specimens treated with the Kolsterisation® process. Note that data points are sufficiently close together that several are at least partially obscured.

Fig. 16. As-received/untreated CD3MN specimen (actual diameter = 16 mm) following sonication for 6 h (2 mm depth) in mercury. Note the slight general roughness with no pitting.

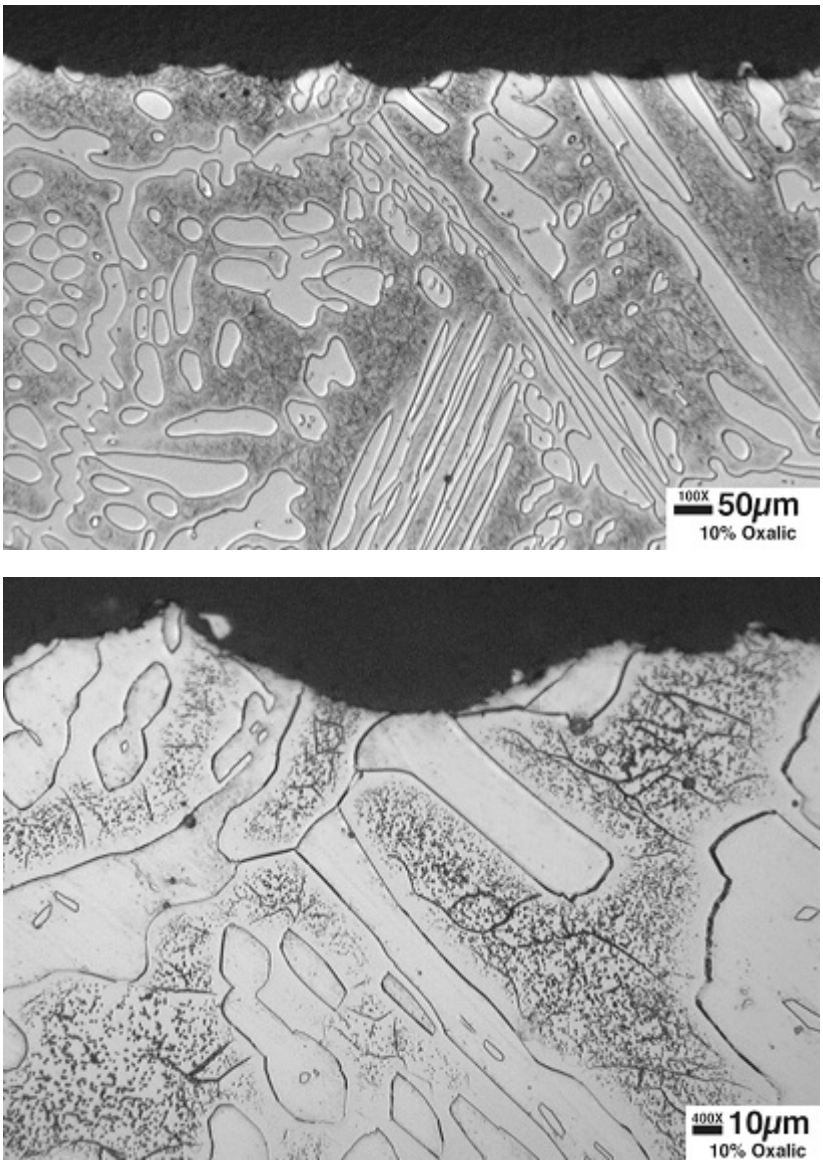

Fig. 17. Cross section of untreated CD3MN specimen following sonication in mercury for 6 h. In both views (representing the same general area, higher magnification at bottom), the specimen surface meets the black mounting epoxy near the top of the photograph. Austenite and ferrite phases appear to erode at equivalent rates.

In the treated condition, the slope of the weight loss curve is reduced to about 0.7 mg/h, with very little surface roughness and no pitting developing on the test surface. In cross section, the treated specimen exposed 6 h (2 mm depth) is shown in Fig. 18. A satisfactory etching procedure to simultaneously reveal the microstructure and case depth proved elusive, but the case depth (about 12-13 μm) in the austenite phase is faintly visible in the higher magnification photograph of Fig. 18. Close examination of the ferrite phase reveals a band 5 μm wide at the outermost surface with a slightly different appearance than the bulk ferrite; this band is likely related to the case hardening process. A small pit/crack penetrates the ferrite and is arrested by the austenite at the top center of the higher magnification photo in Fig. 18.

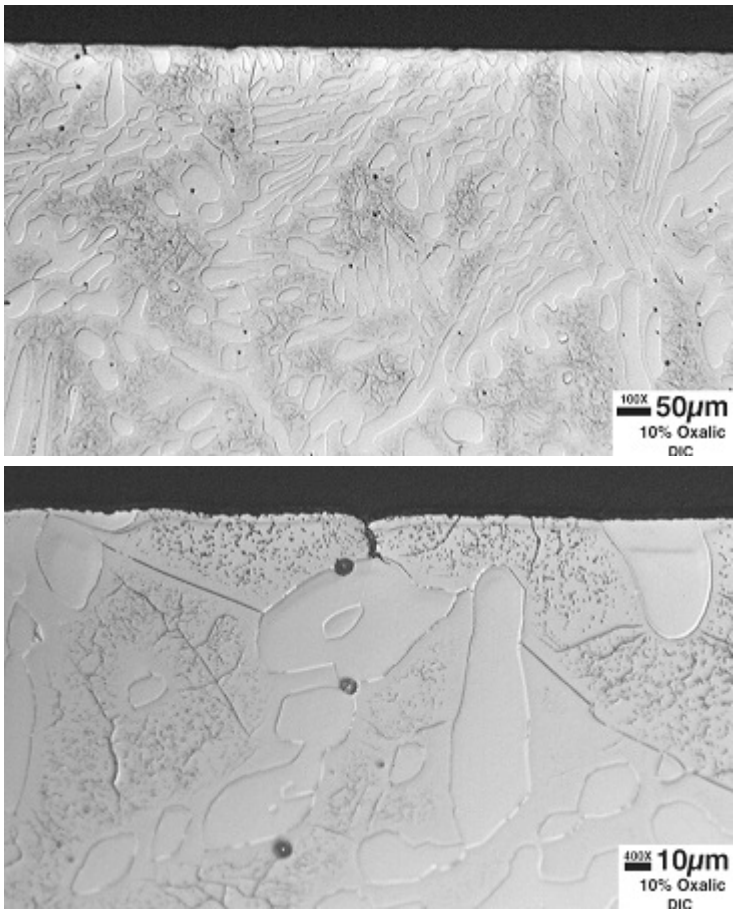

Fig. 18. Cross section of treated CD3MN specimen following sonication in mercury for 6 h. In both views (representing the same general area, higher magnification at bottom), the specimen test surface meets the black mounting epoxy near the top of the photograph.

Microhardness profiles of unexposed portions of this specimen indicate a maximum surface hardness near R_c 60 with a total case depth of about 30 μm. On the exposed test surface, a case thickness closer to 17-20 μm and a maximum hardness near R_c 53 suggests that a portion of the hardened surface has been eroded away during sonication.

One of the untreated CD3MN specimens (subsequently discarded from this analysis), exhibited a very unusual result following the initial sonication exposure. The specimen, which was examined prior to testing and found to be smooth (800 grit finish) and uniform over the entire test surface, was found to exhibit a single, but very large/deep, pit following the first hour of testing (see Fig. 19). Further analysis of the specimen revealed that a very thin surface layer – something similar to a loosely attached "flap" of material – apparently covered this casting pore in the pre-test surface condition. Sufficient erosion or cavitation damage was incurred during the first hour of testing to penetrate/dislodge this "flap" and expose the large, relatively smooth sided, casting pore. The pore penetrated the entire head of the test specimen and opened into the hollow, threaded shank of the test button.

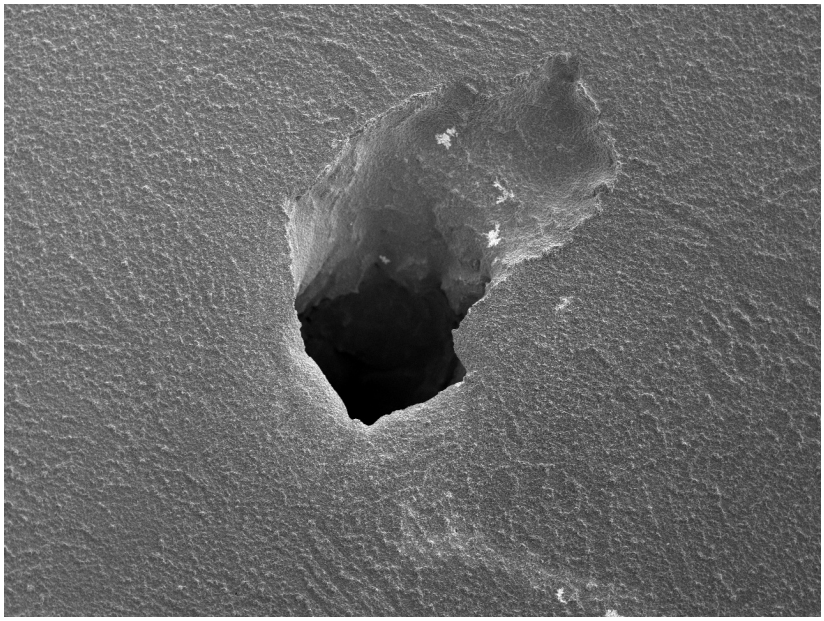

Fig. 19. Photograph of the large, through-pore exposed on the surface of an untreated CD3MN specimen after 1 h sonication in mercury. The actual diameter of the pore (horizontal direction in the photo) is about 0.5 mm.

The through-specimen pit in Fig. 19 was not caused by the cavitation-erosion process, but it does highlight an inherent issue about castings. That is, the potential for porosity is unavoidably an issue with castings, and the pores can result from irregularly spaced gas pockets or shrinkage cavities that meander over significant distances. While these problems are not particularly common in modern casting processes for high alloys, the presence of such pores in the present material points to the need for caution when specifying castings for service where a leak (as a result of such a pore/flaw) could cause mercury to get past seals or other boundaries, thereby causing contamination issues.

3.2.5 CW12MW

This material is a nickel-base alloy similar to the alloy C family of materials, and is expected to exhibit similar good corrosion resistance to a range of chemical environments suitable for highly alloyed nickel. This alloy is the only non-ferrous material included in this study.

Figure 20 summarizes the cavitation-erosion data gathered for CW12MW in this investigation. The slope of the weight loss curve for the untreated specimens tested at the 2 mm immersion (3.5 mg/h) is about 13% higher than the average slope for the untreated specimens tested at the 25 mm depth condition (3.1 mg/h), which is consistent with the difference indicated between these test conditions calculated using total weight loss and profile development in Table 2.

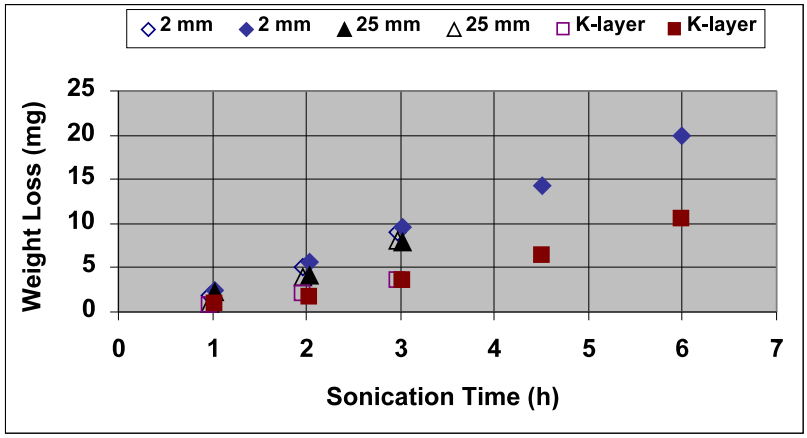

Fig. 20. Weight loss as a function of sonication time in mercury for untreated specimens (2 mm and 25 mm immersion depth) and treated specimens (2 mm immersion depth) of as-cast CD12MW. "K-layer" indicates specimens treated with the Kolsterisation® process. Note that data points are sufficiently close together that several are at least partially obscured.

Figure 21 shows the surface of the untreated specimen following sonication for 6 h (2 mm depth). It reveals a non-uniform surface, with some areas relatively smooth (little profile development) and others yielding the development of pits/craters. The nominal profile development in areas without an obvious crater was determined with the microscope to be about 30 μm for this specimen, with many pits/craters in the range of 75 to 110 μm deep.

Fig. 21. As-received/untreated CW12MW specimen (actual diameter = 16 mm) following sonication for 6 h (2 mm depth) in mercury. Surface reveals non-uniform pitting damage.

Figure 22 shows a representative cross section of the untreated specimen exposed to sonication conditions for 6 h (2 mm depth), and it reveals three pits 50 to 70 μm deep on a nominal profile of about 30 μm between pits. The structure of this alloy is almost wholly austenitic, but there are small precipitates (probably M_6C carbides and possible sigma phase, too) uniformly interspersed. A higher magnification view of the precipitates appears in the lower photograph in Fig. 22.

The cavitation-erosion results for the treated specimen were somewhat mixed. Clearly (Fig. 20 and Table 2), the Kolsterising® treatment reduced weight loss and profile development compared to the untreated condition. However, rather than a constant slope over the short test duration, the average weight loss rate increased from

about 1.4 mg/h early in the test – approximately twice the weight loss rate of 0.7-0.8 mg/h observed for most treated austenitic specimens) – to about 2.9 mg/h at the end of the 6 h exposure. Figure 23 shows a cross section of the treated specimen following sonication for 6 h, and it indicates a remaining surface treatment layer of about 5-8 μm that is periodically breached by a pit.

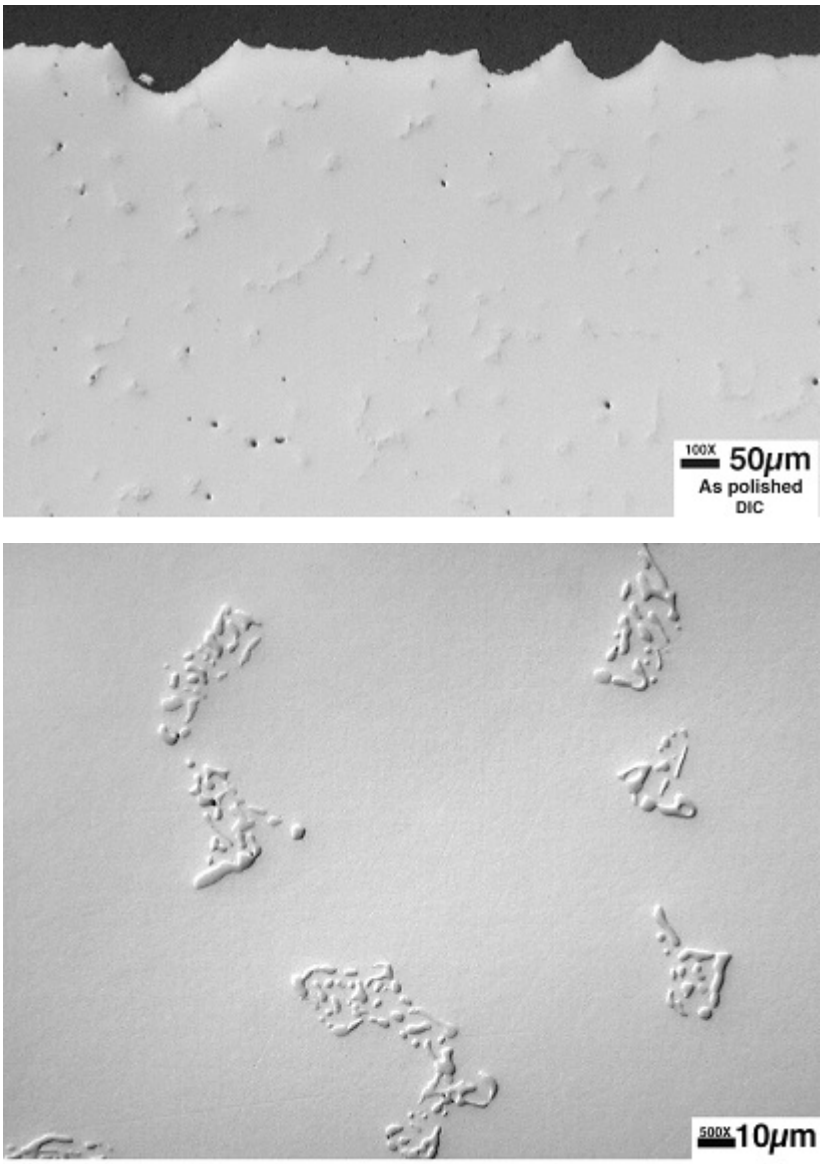

Fig. 22. Cross section of untreated CD12MW specimen following sonication in mercury for 6 h. The test surface is at the top in the top photo (mounting epoxy appears black). At bottom, a higher magnification view (from the central portion of the cross section) of the precipitate phase.

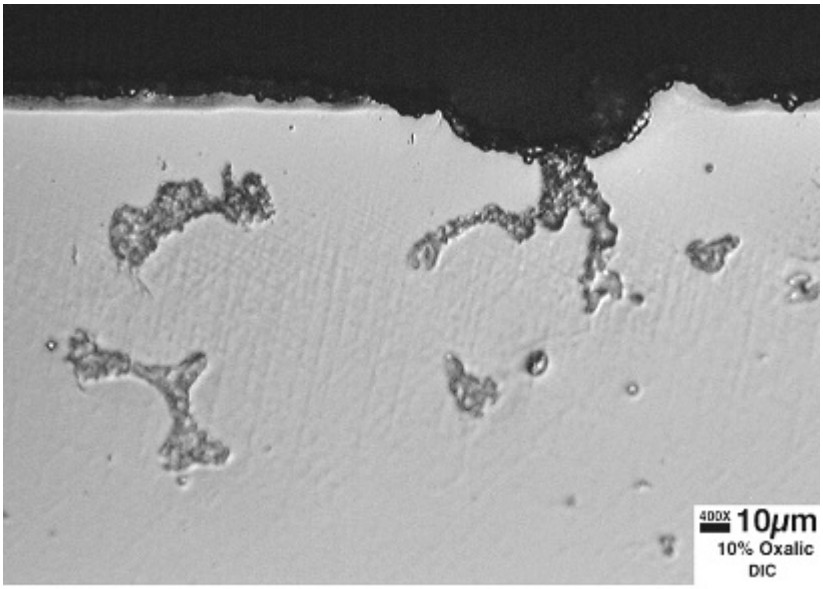

Fig. 23. Cross-section of a treated CW12MW specimen sonicated in mercury for 6 h (2 mm depth). This view shows a region where the surface layer has been breached by a pit.

The microhardness scans reveal a case depth on the unexposed test button surfaces on the order of 30 μm, with a peak hardness approximately R_c 60. However, on the test surface, the microhardness scans indicate only the initial bulk hardness, implying that the hardened layer has been essentially removed by the sonication exposure. This result is consistent with Fig. 23 showing only a very thin case layer, and suggests the high (and increasing) weight loss results from a surface layer that is not as protective as for some other alloys and is more readily breached (at least within the 6 h exposures used here).

3.2.6 HC-600

HC-600 is classified as an abrasion-resistant white cast iron and is covered by ASTM A532 (Class III, type A material). It is a heat-treatable, relatively highly alloyed cast iron capable of developing very high hardness for wear/abrasion service. The material used to make specimens for this investigation was in the as-cast and hardened condition, but the precise hardening treatment was not disclosed to the author. It should also be noted that perhaps this material was not of the highest fundamental quality, as the material provided for machining specimens was in the form of a thick-section (8 cm) gear that had failed in a former service by wholesale brittle intergranular fracture.

Figure 24 summarizes the cavitation-erosion data gathered for specimens of HC-600. Among the untreated specimens, the 25 mm depth condition was actually slightly more aggressive than the 2 mm exposure (unique behavior among the alloys showing good cavitation-erosion resistance). The graph also shows that the performance of the treated and untreated specimens is largely indistinguishable.

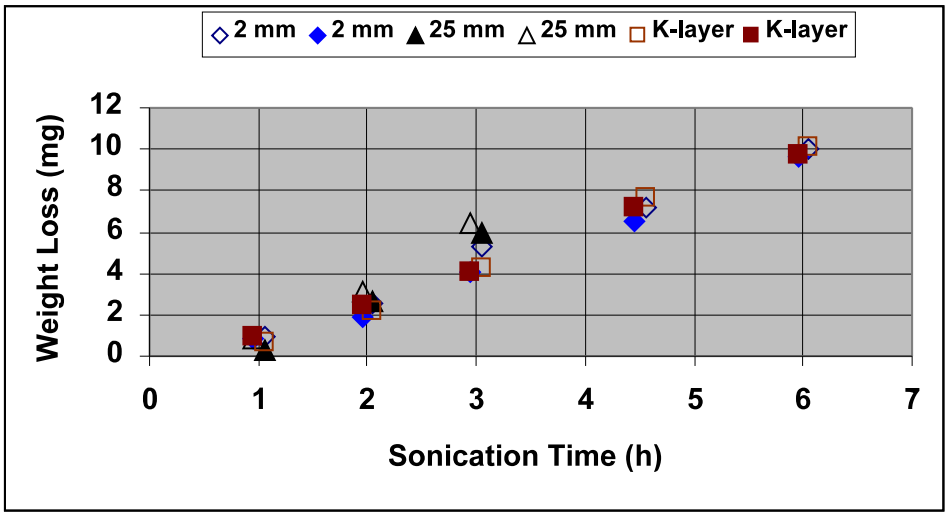

Fig. 24. Weight loss as a function of sonication time in mercury for untreated specimens (2 mm and 25 mm immersion depth) and treated specimens (2 mm immersion depth) of as-cast and hardened HC-600. "K-layer" indicates specimens treated with the Kolsterisation® process. Note that data points are sufficiently close together that several are at least partially obscured.

Figure 25 shows the test surface of an untreated HC-600 specimen sonicated in mercury for 6 h (at the 2 mm depth). Slight discoloration of the test surface among the sonicated specimens was common, and a general surface roughness/profile of about 15 μm was observed following 6 h sonication. In addition, the surface exhibited scattered pitting of the type shown in cross section in Fig. 26. It is possible that many of these pits initiate when interdendritic carbides intersecting the surface are dislodged. Martensite is the matrix phase depicted in Fig. 26 for HC-600.

Fig. 25. As-received/untreated HC-600 specimen (actual diameter = 16 mm) following sonication for 6 h (2 mm depth) in mercury. The test surface shows a general surface roughness of ~15 μm as well as slight discoloration.

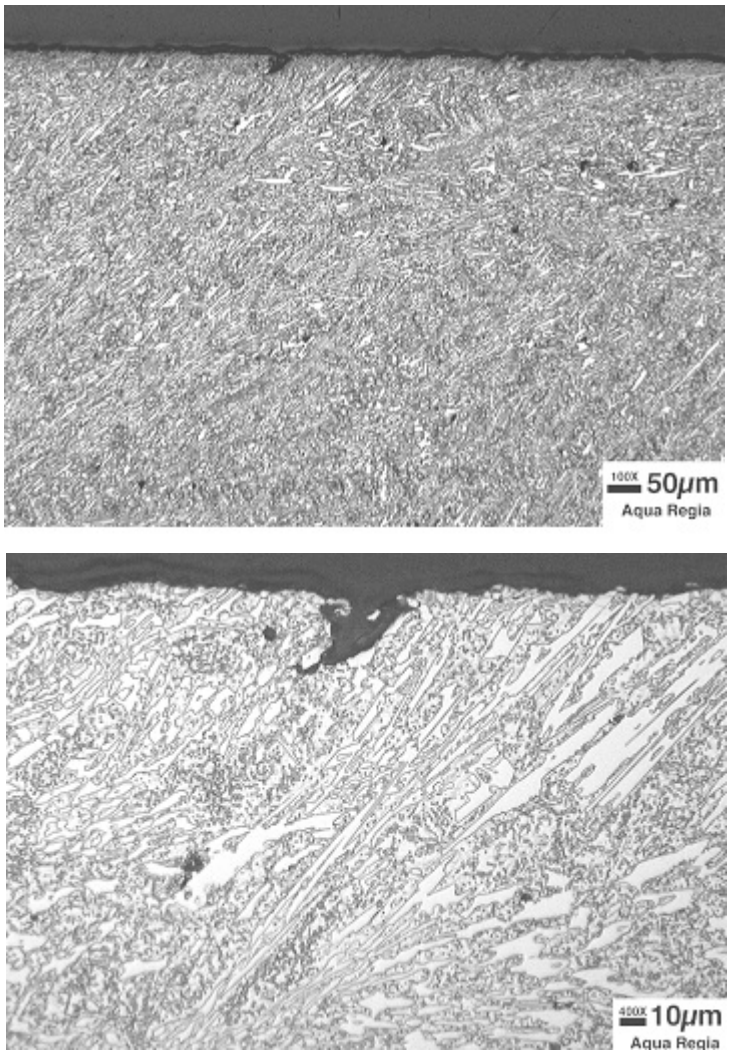

Fig. 26. Cross section of treated HC-600 specimen following sonication for 6 h. In both views (representing the same general area, higher magnification at bottom), the specimen test surface meets the black mounting epoxy near the top of the photograph. The pit shown here mat be associated with interdendritic carbides.

Consistent with the indistinguishable performance of the treated and untreated specimens (2 mm depth), the microhardness scans did not suggest the presence of a hardened layer on the treated specimens. This may be due in part to the fact that the bulk macrohardness is very high, but the microhardness scans near the surface actually indicated a slight decrease in hardness form the bulk value.

3.2.7 Gray Cast Irons

Two gray cast irons of very similar structure and composition were examined in this study, with the difference being a slight strength upgrade from Class 30 to Class 40 material in anticipation that the relative strength might influence cavitation behavior. [The magnitude of the strength upgrade is modest, and is reflected most readily in the relative bulk hardness values in Table 1.] The gray cast irons are relatively inexpensive and commonly used in the as-cast condition when corrosion resistance and mechanical properties are a secondary consideration.

Consistent with the slightly higher strength/hardness, the Class 40 material was observed to be somewhat more resistant to cavitation-erosion than the Class 30 material, but both exhibited a very high weight loss – about an order of magnitude or more higher than the more resistant materials – and substantial profile development. Material removal from these specimens was so extreme during sonication that the surface of the test mercury was found to be discolored with floating oxide/carbide debris just minutes into each 1 h exposure period. In contrast, the “stainless” materials in this test matrix could be tested for many hours with the mercury remaining essentially free of floating debris.

Figure 27, showing a Class 30 specimen following sonication for 3 h (2 mm depth), is representative of the performance of the gray cast irons. The post-test surface exhibited no relatively smooth areas and, rather than individual pits, the surface was a continuous matrix of overlapping craters of variable depth – in this particular case, in the range of 100 to 150 μm. Figure 28 is a representative cross section of this specimen showing the extreme profile development. In some cases, the graphite flakes seemed to be eroding at a slightly accelerated rate compared to the matrix material, but there may be an orientation factor involved as such indications were relatively rare.

The Kolsterizing® treatment did not improve the cavitation-erosion resistance of the gray cast irons and may, in fact, have deteriorated it further. Of some note is that fact that the treated specimens exhibited swelling of the button dimensions as a result of the treatment – approximately 5% – which necessitated significant effort to clean/rework the threads on each button. During this effort, one button of each gray cast iron material was sheared apart (very brittle failure) at the junction of the test head and threaded shank during thread repair. The effect on the results of a slightly “swollen” test surface is not clear, but the extreme stress in the surface layers probably contributed to rapid spallation of carburized material.

Fig. 27. As-received/untreated Class 30 gray cast iron specimen (actual diameter = 16 mm) following sonication for 3 h (2 mm depth) in mercury. Compared to other similar photos in this report, this one is at more of an angle to reveal the overlapping craters in the profile.

3.2.8 Ni-resist

Ni-resist has something of a reputation as an erosion resistant cast iron, but the specific composition (and heat treatment) of the alloy tested here was not selected for optimized resistance to mercury but was among the materials readily available from a supplier. [It is the author's opinion that a higher alloy content, particularly in chromium and manganese, would be required for this alloy to develop greater cavitation-erosion resistance, but multiple efforts to find such a material were not fruitful.]

The Ni-resist material essentially disintegrated in the sonication test. In terms of weight loss and profile development in a 3 h exposure, this material exhibited the highest value in each category by a significant margin. Macroscopically, the post-test appearance of the Ni-resist specimens was indistinguishable from the gray cast irons except that the depth of the profile was significantly greater. Figure 29 shows a representative cross section of an untreated Ni-resist specimen (3 h test, 2 mm depth). Note in particular the relatively brittle nature of this alloy's performance in the cavitation test (piece of material broken loose near the mouth of a pit).

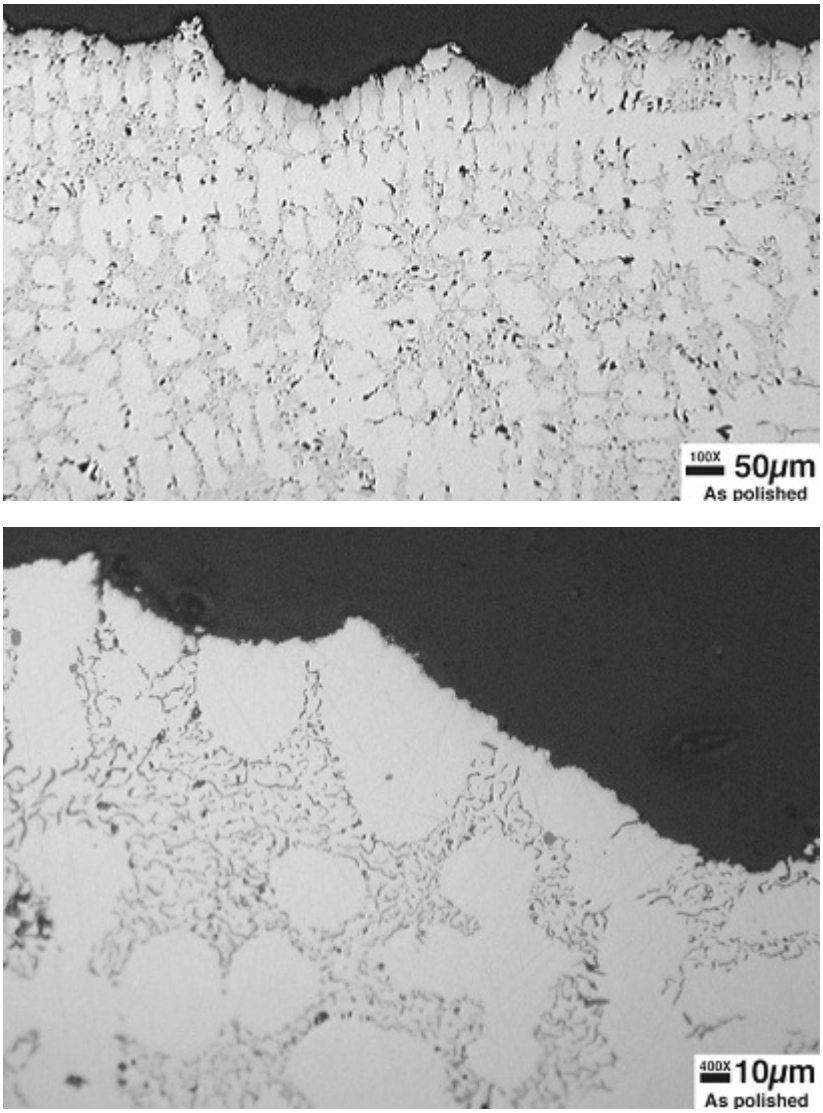

Fig. 28. Cross section of untreated Class 30 gray cast iron specimen following sonication in mercury for 3 h. In both views (representing the same general area, higher magnification at bottom), the specimen test surface meets the black mounting epoxy near the top of the photograph. These photographs reveal extensive profile development.

Fig. 29. Cross section of untreated Ni-resist cast iron specimen following sonication in mercury for 3 h. The specimen test surface meets the black mounting epoxy near the top of the photograph. Note the piece of material that appears ready to break from the surface near the mouth of the pit.

Like the gray cast irons, the Kolsterizing® treatment did not improve the cavitation-erosion resistance of the Ni-resist specimens. Like the gray cast irons, however, significant swelling of the test button as a result of the treatment process was also observed.

4. CONCLUSIONS

The vibratory horn was used as a screening tool to assess the relative cavitation-erosion resistance of a series of cast materials potentially suitable for use as pump impellers for mercury service. In the as-cast condition, HC-600 and CD3MWCuN were the most resistant alloys based on minimum weight loss and profile development. Several other alloys, including CA-15, CD3MN, CW12MW, and CF8M also exhibited superior performance in the as-cast condition to the reference alloy (wrought annealed 316LN stainless steel), but were not as resistant to cavitation in mercury as the best alloys examined. Three different cast iron materials (Class 30 and Class 40 gray cast irons and Ni-resist) exhibited very poor cavitation-erosion resistance in mercury and should not be considered for this service.

Test specimens of the as-cast materials were also subjected to a low temperature carburizing treatment intended to case-harden the alloy surfaces thereby increasing cavitation-erosion resistance. Following this treatment, CD3MN and CD3MWCuN yielded the lowest weight loss and profile development, although several other alloys also responded positively to the surface hardening treatment and exhibited performance superior (to variable degree) to their untreated counterparts. HC-600 was sufficiently hard in the as-cast condition that the surface hardening treatment essentially had no effect on the cavitation resistance, and the hardening treatment seemed to degrade the cavitation resistance of the cast irons.

The overall results tend to suggest the best alloy among those examined, based on minimum weight loss and pitting, in both the as-cast condition as well as the surface hardened condition, was CD3MWCuN. However, several other alloys were also found generally resistant to the cavitation conditions created in the vibratory horn test and are likely to provide satisfactory service as impeller materials in mercury service, too. Ultimately, material cost, availability, and vendor scheduling factors could prove to be deciding factors for material selection for pump impellers among several satisfactory possibilities. As highlighted by a casting pore that completely penetrated one of the test specimens, appropriate quality control and inspection of cast materials should be included in any design/purchase specifications.

5. ACKNOWLEDGMENTS

The author gratefully acknowledges the contribution of several other individuals to this research and report. Funding for this effort was provided by D. C. Lousteau from the Spallation Neutron Source Project at Oak Ridge National Laboratory, as were some of the test materials. H. F. Longmire performed the metallography of the post-test specimens as well as the microhardness evaluations, and T. Brummett provided the scanning electron micrographs. L. K. Mansur and D. F. Wilson reviewed the manuscript. F. C. Stooksbury helped prepare and distribute the manuscript.

6. REFERENCES

1. S. J. Pawel and E. T. Manneschmidt, “Preliminary Evaluation of Cavitation Resistance of Tyle 316LN Stainless Steel in Mercury Using a Vibratory Horn,” **J. Nucl. Mater.**, 318 (2003) 122-131.

2. S. J. Pawel, “Assessment of Cavitation-Erosion Resistance of 316LN Stainless Steel in Mercury as a Function of Surface Treatment,” **J. Nucl. Mater.**, 343 (2005) 101-115.

3. Standard Test Method for Cavitation Erosion Using Vibratory Horn Apparatus, ASTM G32-98, American Society for Testing and Materials, Philadelphia, PA, 1998.

4. S. J. Pawel and L. K. Mansur, “Evaluation of Cavitation-Erosion Resistance of 316LN Stainless Steel in Mercury Containing Metallic Solutes,” Oak Ridge National Laboratory Report, **ORNL/TM-2006/539** (August 2006).

5. K. Farrell, et. al, “Characterization of a Carburized Surface Layer on an Austenitic Stainless Steel,” **J. Nucl. Mater.**, 343 (2005) 123-133.

INTERNAL DISTRIBUTION

1. P. J. Blau
2. D. C. Lousteau
3. L. K. Mansur
4. T. J. McManamy
6-8. S. J. Pawel
9. B. W. Riemer
10. P. F. Tortorelli
11. M. W. Wendel
12. D. F. Wilson
13. S. J. Zinkle
14. Central Research Library
15. ORNL Laboratory Records–RC